



A Model for Inelastic Deformation of Irradiated Zirconium Alloy Cladding under Transient Conditions

Lars Olof Jernkvist

Luleå University of Technology, Sweden

ABSTRACT

This paper presents a constitutive model for inelastic deformation of zirconium alloy cladding in light water reactor fuel rods. The model belongs to the class of generalised standard materials, and it is based on the theory of thermodynamics with internal state variables. From this theory, an anisotropic viscoplastic law with combined isotropic and kinematic hardening is derived, in which effects of irradiation and static recovery are included. The model is intended for prediction of cladding creep and viscoplasticity under transient reactor conditions, and has been calibrated with experimental in-reactor and out-of-reactor data taken from literature.

1. INTRODUCTION

Zirconium alloys are used in cladding tubes for light water reactor fuel rods, owing to their mechanical strength, resistance to corrosion and small cross section for neutron capture [1]. Due to intense neutron exposure, elevated temperature and stress, the cladding tubes undergo inelastic deformation under operation. The deformation may under stress-free conditions result from irradiation-induced growth and zirconium-water reactions [2]. These processes are slow, and will not be treated in this paper, where we will focus on inelastic deformation under stress. In this context, a distinction is made between viscoplasticity and creep. The first term is used when applied stresses exceed the material yield strength, whereas creep is active also at stresses below the yield limit. In the cladding tubes, both viscoplasticity and creep are believed to be manifested through a combined dislocation glide-climb process, where climb is rate-controlling for the creep deformation [3].

In fuel rod design and safety analyses, there is an obvious need to predict the cladding inelastic deformation, since it affects the fuel rod heat transfer and may also induce dimensional changes to the fuel assemblies. The predictions of zircaloy in-reactor creep and viscoplastic deformation are complicated by the material anisotropy and the large spread in yield strength between materials which have undergone different heat treatments under manufacture, but also by changes in material properties that are induced by irradiation. Incident energetic particles, mainly fast neutrons, generate vacancy and interstitial point defects. Part of these defects aggregate and form clusters, that restrict dislocation movements and thus result in an increased yield strength [4]. The irradiation also causes a pronounced creep enhancement, which is believed to be due to the generation of mobile point defects that promote the rate-controlling climb component of the creep deformation [5].

Thus, the inelastic deformation behaviour of zirconium alloy cladding materials is strongly dependent on both the manufacturing process and the operational environment. For this reason, the predictive capability of material models is generally restricted to a certain cladding material and to a limited range of operational conditions. Although very accurate within their range of application, these models are generally not suited for analyses of inelastic deformation under off-normal conditions, such as pellet-cladding interaction or power-cooling mismatch events, where rapid changes of temperature and/or stress state are involved. Transient creep models, specifically intended for this kind of problems, usually comprise a set of state variables that defines the momentary internal structure of the material [6,7]. Changes of the material inelastic behaviour under complex time histories are modelled by the evolution of these variables, which are generally related to the material hardening. The model proposed in this paper follows this concept, and a system of coupled evolution equations for inelastic strain and internal state variables is derived from fundamental thermodynamic principles and adapted to irradiated zirconium alloy materials.

2. FUNDAMENTAL THERMODYNAMIC PRINCIPLES

In the presented model, changes in material properties due to deformation, irradiation and heating are described by the evolution of a set of appropriately chosen internal state variables. The evolution of these variables has to comply to the first and second principle of thermodynamics, which are usually cast in the form of the Clausius-Duhem inequality,

$$\boldsymbol{\sigma} : \dot{\boldsymbol{\epsilon}} + U - \rho(\dot{\Psi} + s\dot{T}) - \frac{1}{T}\mathbf{q} \cdot \nabla T \geq 0 . \quad (1)$$

Here, ρ , $\boldsymbol{\sigma}$, $\boldsymbol{\epsilon}$, s , T , \mathbf{q} , and Ψ are the density, stress, strain, specific entropy, temperature, heat flux and Helmholtz free energy. U denotes the part of the power input from irradiation, which is stored in the material in the form of irreversible changes to the microstructure, e.g. through nucleation of point defect clusters [8]. Assuming now that Ψ is a function of the elastic strain, temperature and a set of internal state variables, \mathbf{a} , we get

$$\boldsymbol{\sigma} : \dot{\boldsymbol{\epsilon}}^{ne} + U - \mathbf{A} \cdot \dot{\mathbf{a}} - \frac{1}{T}\mathbf{q} \cdot \nabla T \geq 0 \quad (2)$$

where $\dot{\boldsymbol{\epsilon}}^{ne}$ is the nonelastic strain rate from creep and viscoplasticity and

$$\mathbf{A} = \rho \frac{\partial \Psi}{\partial \mathbf{a}} \quad (3)$$

are thermodynamic variables, associated to the internal state variables \mathbf{a} . Eq. (2) constitutes a general condition that has to be fulfilled by any constitutive model, formulated on the basis of internal state variables. Now, considering the irreversible power input from irradiation, U , we make the assumption that it is proportional to the fast neutron flux, $U = \mu \dot{\phi}$, where μ is the average linear energy transfer to the irreversible microstructural damage processes.

Fulfilment of the dissipation inequality in eq. (2) is then secured by applying Fourier's law as the constitutive relation for heat conduction, and using the concept of a generalised standard material [9], whereby $\dot{\boldsymbol{\epsilon}}^{ne}$, μ and the evolution of internal state variables are derived from a convex function φ^* through the normality rule

$$\dot{\boldsymbol{\epsilon}}^{ne} = \frac{\partial \varphi^*}{\partial \boldsymbol{\sigma}} \quad \mu = \frac{\partial \varphi^*}{\partial \dot{\phi}} \quad \dot{\mathbf{a}} = - \frac{\partial \varphi^*}{\partial \mathbf{A}} . \quad (4)$$

Here, $\varphi^*(\boldsymbol{\sigma}, \dot{\phi}, \mathbf{A})$ is the dual dissipation potential. It has to be a non-negative convex function, which is zero at the origin ($\boldsymbol{\sigma} = \dot{\phi} = \mathbf{A} = 0$).

3. MODEL FORMULATION

The concept of generalised standard materials provides a basis upon which physically admissible material models can be formulated. Such a formulation firstly requires that a set of state variables, \mathbf{a} , and associated thermodynamic variables, \mathbf{A} , are identified. Secondly, analytical expressions for the Helmholtz free energy and the dual dissipation potential must be specified in terms of these variables, so that changes in material properties under inelastic deformation, heating and irradiation are properly represented by the laws in eqs. (3) and (4).

3.1 Axial symmetry and material orthotropy

Due to the axial symmetry of the cladding tubes, only four components of the stress and strain tensors need be considered. Henceforth, a four-component Voigt-notation will be used:

$$\boldsymbol{\sigma} = (\sigma_r, \sigma_z, \tau_{rz}, \sigma_\theta) \quad \text{and} \quad \boldsymbol{\varepsilon} = (\varepsilon_r, \varepsilon_z, \gamma_{rz}, \varepsilon_\theta) . \quad (5)$$

The texture-induced anisotropy of the cladding material is considered by using an equivalent stress defined by

$$\sigma_{eq}(\boldsymbol{\sigma}) = \sqrt{\frac{3\boldsymbol{\sigma}' \cdot \mathbf{M} \cdot \boldsymbol{\sigma}'}{2}} , \quad (6)$$

where $\boldsymbol{\sigma}'$ is the deviatoric stress vector and the symmetric rank 2 tensor \mathbf{M} is dependent on the material texture and the preference for slip in certain crystallographic directions. For a certain cladding material, \mathbf{M} can be determined experimentally, but approximate analytical expressions for \mathbf{M} are also available [6]. In the model, the texture induced anisotropy is assumed to be unaffected by temperature and inelastic deformation, which restricts the applicability to small inelastic strains and temperatures below 1100K.

3.2 Selection of internal state variables

The anisotropy connected with inelastic deformation of zirconium alloy cladding is not only due to the material texture, but also to kinematic hardening (Bauschinger effect). This flow-induced anisotropy is considered by introducing a tensorial internal state variable, \mathbf{x} , which corresponds to kinematic hardening. In the same way, two scalar state variables, r_d and r_r , are selected for representation of isotropic hardening due to inelastic deformation and irradiation respectively. The thermodynamic variables associated to r_d , r_r and \mathbf{x} will be denoted R_d , R_r and \mathbf{X} . They represent an isotropic increase of the yield strength and a back stress respectively, and are derived from eq. (3).

3.3 The Helmholtz free energy function

The Helmholtz free energy may be written in a partitioned analytical form,

$$\Psi(\boldsymbol{\varepsilon}^e, T, r_d, r_r, \mathbf{x}) = \Psi^e(\boldsymbol{\varepsilon}^e, T) + \Psi^{ne}(r_d, r_r, \mathbf{x}, T) , \quad (7)$$

where the elastic part Ψ^e is given by Duhamel-Neumanns form of Hookes law of elasticity,

$$\Psi^e = \frac{1}{2\rho} \boldsymbol{\varepsilon}^e \cdot \mathbf{C} \cdot \boldsymbol{\varepsilon}^e - \frac{\alpha}{\rho} (T - T_0) \boldsymbol{\varepsilon}^e . \quad (8)$$

Here, \mathbf{C} is the rank 2 isotropic elasticity tensor and α is a scalar constant. The inelastic part is

$$\Psi^{ne} = \frac{r_d^2 + r_r^2}{2\rho} + \frac{2H_2}{9\rho} \sigma_{eq}^2(\mathbf{x}) , \quad (9)$$

where H_2 is a model parameter.

3.4 The dual dissipation potential

A partitioned analytical form is assumed also for the dual dissipation potential,

$$\phi^* = \Omega_p(\sigma_p, T) + \Omega_c(\sigma_c, T, \dot{\phi}) + \Omega_a(R_d, R_r, T) + \Omega_r(R_r, \dot{\phi}), \quad (10)$$

where the subscripts p , c , a and r allude to effects of plasticity, creep, annealing and radiation. This partitioning is convenient, since it allows separate but mutually interacting models to be developed for these four dissipative processes. The arguments σ_p and σ_c are given by

$$\sigma_p = \frac{\sigma_{eq}(\sigma - X)}{(k + R_d + R_r)} \quad \text{and} \quad \sigma_c = \frac{\sigma_{eq}(\sigma - X)}{(1 + \beta R_r/k)} \quad (11)$$

where k is the yield stress of the material in its fully recrystallised state, and β is a parameter.

3.5 The final model

The analytical form of each term in eq. (10) can be chosen freely from the class of non-negative convex functions, so that the evolution of internal state variables given by eq. (4) becomes representative for the true material behaviour [9]. In our model, the chosen functions result in the following evolution equations for inelastic deformation and hardening:

$$\dot{\epsilon}^p = \frac{3\dot{p} \mathbf{M} \cdot (\boldsymbol{\sigma}' - \mathbf{X}')}{2\sigma_{eq}(\boldsymbol{\sigma} - \mathbf{X})} \quad \text{and} \quad \dot{\epsilon}^c = \frac{3\dot{c} \mathbf{M} \cdot (\boldsymbol{\sigma}' - \mathbf{X}')}{2\sigma_{eq}(\boldsymbol{\sigma} - \mathbf{X})} \quad (12)$$

$$\dot{R}_d = - e^{-Q_d/T} \left(\frac{R_d}{A_1} \right)^2 \quad (13)$$

$$\dot{R}_r = R_1 \dot{\phi} (R_{\infty} - R_r) \ln^{-3} \left(\frac{1}{1 - R_r/R_{\infty}} \right) - \frac{e^{-Q_r/T}}{\ln(R_{\infty}/R_r)} \frac{R_r}{A_2} \quad (14)$$

$$\dot{X} = \frac{2H_2}{3} \mathbf{M} \cdot (\dot{\epsilon}^p + \dot{\epsilon}^c) - \frac{D(\dot{p} + \dot{c})(1 + R_r/k)}{(\sigma_{eq}(\boldsymbol{\sigma}) + k)} \mathbf{M} \cdot \mathbf{M} \cdot \mathbf{X} . \quad (15)$$

Here, $\dot{\epsilon}^p$ and $\dot{\epsilon}^c$ are inelastic strain rates from viscoplasticity and creep. Other introduced parameters are given in table 4.1. The nonelastic strain is split into contributions from viscoplasticity and creep, since different deformation mechanisms are believed to be operative at high and low stress, and the effect of annealing on the inelastic deformation rate is more easily considered by this separation. The effective viscoplastic strain rate is given by

$$\dot{p}(\sigma_p, T) = P_1 \left(e^{P_2 \langle \sigma_p^{-1} \rangle} - 1 \right) \quad (16)$$

where $\langle \rangle$ are the McCauley brackets, and P_1 and P_2 are temperature dependent parameters presented in table 4.1. The effective creep strain rate is calculated from an additive creep law

$$\dot{c}(\sigma_c, T, \dot{\phi}) = C_1 e^{-Q_c/T} \sinh^{C_3}(C_2 \sigma_c) + C_4 \dot{\phi}^{0.85} \sigma_c \quad (17)$$

where the model parameters C_i are given in table 4.1. The first term in eq. (17) is related to thermal creep, where Q_c is the creep activation energy divided by the molar gas constant, whereas the second term gives the athermal creep contribution from irradiation.

The annealing involves high-temperature recovery of lattice defects, which annihilates prior isotropic and kinematic hardening. The defects caused by irradiation are generally smaller and more easily dissolved than dislocation loops induced by inelastic deformation [10], and irradiation hardening is therefore much faster recovered under annealing than deformation hardening.

As can be seen from eq. (13), isotropic deformation hardening is neglected, and only softening due to static recovery is considered. This is in accordance with experimental observations on zirconium alloy behaviour under moderate inelastic deformation and normal operating temperatures [11]. From the expression in eq. (11) for the reduced stress applied in the viscoplastic correlation, we see that the contributions to isotropic hardening from deformation and irradiation are assumed to be additive. However, these two forms of isotropic hardening are treated as independent phenomena, due to the large difference in recovery rate under annealing. The kinematic deformation hardening is strongly coupled to irradiation. As can be seen from the last term of eq. (15), the dynamic recovery rate of X increases with irradiation hardening, R_r .

4. MODEL CALIBRATION

The introduced model parameters have been fitted to experimental data taken from literature, and the considered experiments include several investigations, in which materials with differing heat treatments are compared with respect to their inelastic deformation behaviour. Most of the tests were performed under steady-state conditions, i.e. under constant temperature and stress. Static recovery experiments performed under stress-free conditions were also included, in order to verify the models ability to simulate annealing.

All the experiments were performed on tubular cladding specimens, which in most cases were subjected to a fixed biaxial stress state $(\sigma_\theta / \sigma_z) = 2$ by internal pressurisation. Since the in-reactor tests were exclusively of this kind, the influence of irradiation on cladding anisotropy could not be characterised. For this reason, the anisotropy tensor \mathbf{M} was assumed to be unaffected by irradiation, which is in accordance with analyses of in-reactor creep [12], although there is some evidence that irradiation attenuates the anisotropy in the high stress regime [13]. The model parameters were determined from experimental data in three steps, where out-of-reactor, in-reactor, and recovery tests were used in the respective step. Table 4.1 presents best-estimate parameter values, which give a reasonable predictability of the material behaviour within the domain covered by the experiments, i.e. for temperatures from 570 to 800 K, inelastic strain rates between 10^{-13} and 10^{-4} s $^{-1}$ and fast neutron fluxes up to $6.3 \cdot 10^{17}$ nm $^{-2}$ s $^{-1}$. The experimental database for the upper part of this domain is meagre, and consequently, the accuracy of the model is expected to decrease with increasing temperature and strain rate.

Table 4.1 Best-estimate model parameter values.

Creep:	Annealing:
$C_1 = 1.43 \cdot 10^8 \text{ s}^{-1}$	$A_1 = 3.14 \cdot 10^{-5} \text{ (Pa s)}^{0.5}$
$C_2 = 1.06 \cdot 10^{-8} \text{ Pa}^{-1}$	$A_2 = 7.43 \cdot 10^{-11} \text{ s}$
$C_3 = 2.13 \text{ -}$	$Q_d = 40000 \text{ K}$
$C_4 = 1.00 \cdot 10^{-33} \text{ (Pa s)}^{-1} (\text{m}^2 \text{ s})^{0.85}$	$Q_r = 23700 \text{ K}$
$Q_c = 24175 \text{ K}$	
Irradiation hardening:	Deformation hardening:
$R_I = 1.12 \cdot 10^{-26} \text{ m}^2$	$H_2 = 1.50 \cdot 10^{10} \text{ Pa}$
$R_{r\infty} = 3.90 \cdot 10^8 \text{ Pa}$	$D = 4.50 \cdot 10^{10} \text{ Pa}$
$\beta = 0.40 \text{ -}$	
Viscoplasticity:	
$P_1 = 6.60 \cdot 10^{-7} \text{ s}^{-1}$	
$P_2 = \begin{cases} 86.0 & T \leq 500\text{K} \\ 0.14e^{3210/T} & T > 500\text{K} \end{cases}$	$k = \begin{cases} 6.02 \cdot 10^8 - 1.44 \cdot 10^6 T + 1.01 \cdot 10^3 T^2 & T \leq 713\text{K} \\ 8.87 \cdot 10^7 & T > 713\text{K} \end{cases} \text{ Pa}$

5. RESULTS AND DISCUSSION

The model was calibrated to experimental data pertaining to materials with disparate chemical composition and thermomechanical treatment, and a common set of model parameters was determined without discriminating the materials. Differences in inelastic behaviour between the materials in their unirradiated state are thus reflected only in the initial values of the hardening variables R_d and X , and also in the anisotropy tensor M . In a fully recrystallised material, R_d and X are both initially zero. For other materials, the initial values can be derived from tensile tests by use of the presented model (inverse problem).

In the experimental database, differences in measured steady-state out-of-reactor creep rates of 50% or more were found also for materials with identical chemical composition, heat treatment, yield strength and texture. Such differences cannot be accounted for by the model, and thus the model parameters have to be tuned to a specific material, if accurate predictions of steady-state creep rates are needed. However, the presented model is primarily intended for analysis of creep and viscoplasticity under reactor transients, and should be judged with respect to its capacity to capture the inelastic deformation under time varying conditions.

As a first example of the model predictability, we use the out-of-reactor creep experiment by Matsuo [14], in which cold-worked stress-relieved Zr-4 cladding was subjected to varying temperature and stress histories. The tubular specimens had an inner diameter of 9.48 mm and a wall thickness of 0.62 mm. The specimens were loaded by internal/external overpressure, resulting in a fixed biaxial stress state ($\sigma_\theta / \sigma_z = 2$).

In figure 1, measured hoop creep strain is compared with model predictions for a cyclic stress history under constant temperature. The histories of applied hoop stress (MPa) and temperature (K) are given at the top of the figure.

Figure 2 shows the result of another test case, in which both the stress and temperature were changed with time. As can be seen from these figures, the very fast transient creep following stress reversal is fairly well predicted by the model. The effect is accounted for solely by the kinematic hardening variable.

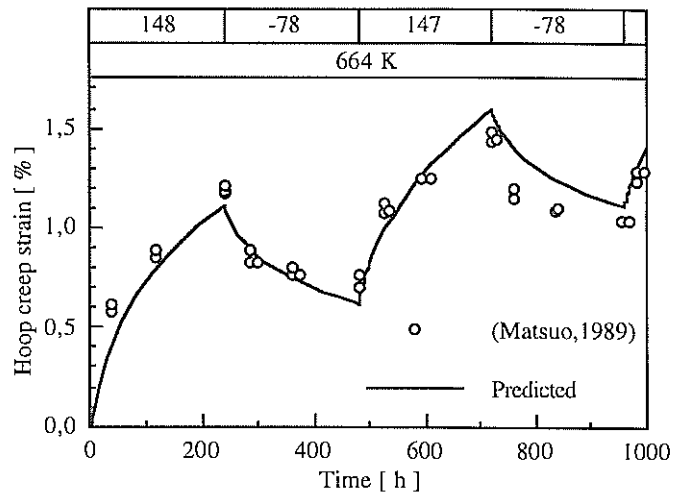


Fig 1. Isothermal stress reversal creep test.

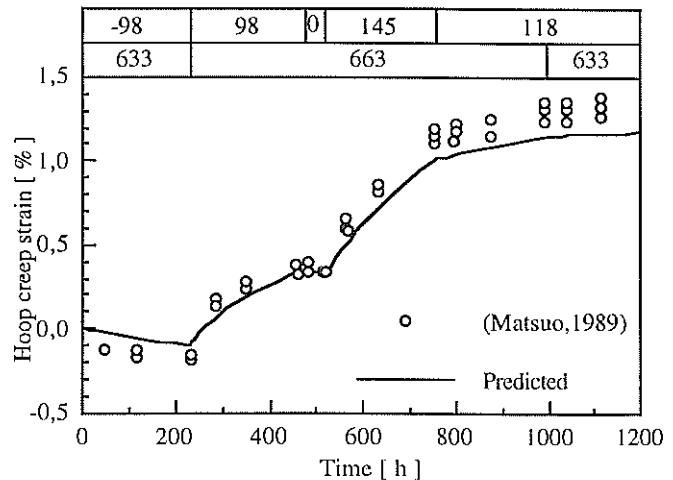


Fig 2. Variable stress and temperature creep test.

A similar transient creep experiment has recently been performed in-reactor at the Halden test reactor in Norway [15]. A test specimen of fully recrystallised Zr-2 material was taken from a water rod, irradiated in a commercial reactor to a fast fluence of $6 \cdot 10^{25} \text{nm}^{-2}$ ($>1 \text{ MeV}$). The tubular specimen, with an inner diameter and wall thickness of 13.48 and 0.76 mm, was placed in the test reactor and subjected to a varying internal pressure history under more than 14000 hours. On-line diameter measurements were made throughout the test, in which the cladding temperature was held in the interval from 573 to 593 K, and the average fast neutron flux was $3.2 \cdot 10^{17} \text{nm}^{-2}\text{s}^{-1}$.

Figure 3 shows the measured inelastic deformation together with predicted hoop creep strain. In this test, only a moderate transient creep is observed upon stress reversal. This is captured by the model, since the kinematic hardening is assumed to decrease due to the irradiation.

As a last example, we study the loss of material strength obtained under a short term temperature excursion, thought to be representative of a dryout event in a boiling water reactor. The considered material is recrystallised Zr-2, which has obtained a fast neutron fluence of $2.5 \cdot 10^{25} \text{nm}^{-2}$. The material is exposed to a fast neutron flux of $4.5 \cdot 10^{17} \text{nm}^{-2}\text{s}^{-1}$ when the temperature is suddenly raised from 563 to 873 K for 30 seconds under a transient.

Figure 4 shows the predicted evolution of the irradiation hardening variable R_r under and after the temperature excursion. Under the transient, the material yield strength decreases with 100 MPa, which is in good agreement with experimental observations by Torimaru *et al.* [10]. Furthermore, it is predicted that approximately four months of full power operation is needed for the cladding material to totally regain its prior yield strength. This long period of operation with a low-strength material may have significant importance to the fuel post-dryout performance.

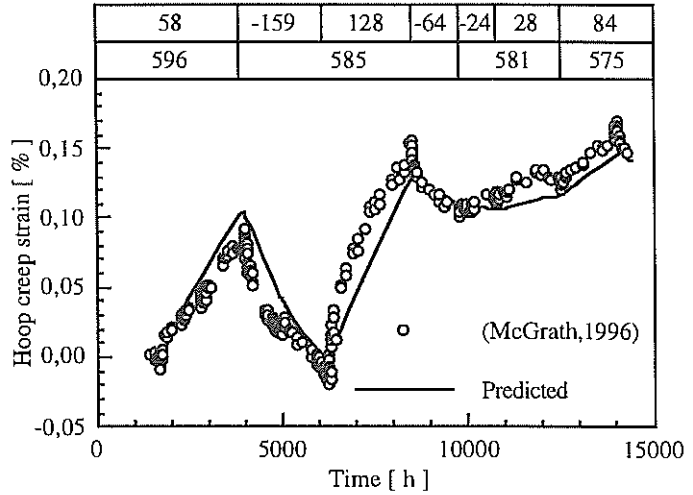


Fig 3. Halden in-reactor stress reversal creep test.

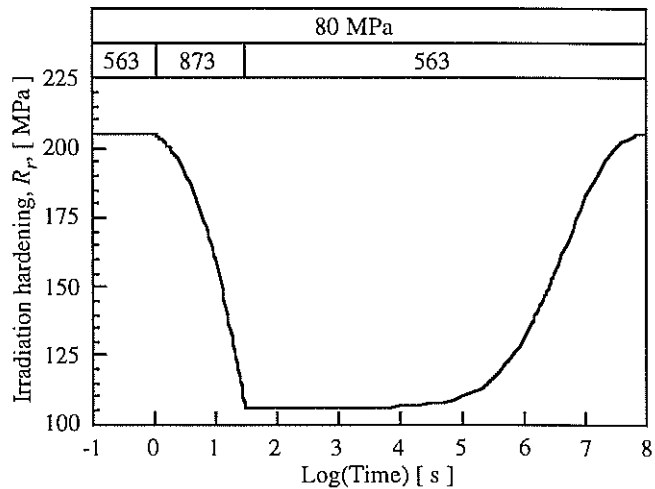


Fig 4. Simulation of irradiation annealing.

6. CONCLUSIONS

A model for combined creep and viscoplasticity in zirconium alloy cladding tubes has been derived within the framework of thermodynamics with internal state variables. It belongs to the class of generalised standard materials, and thus satisfies the thermodynamic constraint of intrinsic dissipation. The model is intended for analysis of cladding inelastic deformation under transient conditions, and has been calibrated to experimental data for recrystallised as well as cold worked cladding materials. Comparisons with both out-of-reactor and in-pile experiments confirm that the transient creep behaviour under varying stress and temperature histories is captured by the model. However, the accuracy in predicted steady-state creep rate is generally poor, unless the model is recalibrated to the specific cladding material under consideration.

The concept of internal state variables leads to a system of coupled equations for the inelastic strain and a set of hardening variables, which are related to the material microstructure and lattice defect density. This modular structure makes it fairly easy to modify and extend the model, so that additional effects can be accounted for within the same framework.

7. REFERENCES

- [1] C. Lemaignan, A.T. Motta, "Zirconium alloys in nuclear applications", *Materials Science and Technology*, Vol 10B, 1994, pp 1-51, VCH Verlagsgesellschaft mbH, Weinheim, Germany.
- [2] V. Fidleris, R.P. Tucker, R.B. Adamson, "An overview of microstructure and experimental factors that affect growth behavior of zirconium alloys", ASTM STP 939, American Society for Testing and Materials, 1987, pp 49-85.
- [3] D.G. Franklin, G.E. Lucas, A.L. Bement, *Creep of zirconium alloys in nuclear reactors*, ASTM STP 815, American Society for Testing and Materials, 1983.
- [4] B.N. Singh, S.J. Zinkle, "Influence of irradiation parameters on damage accumulation in metals and alloys", *J. Nucl. Mat.* Vol 217, 1994, pp 161-171.
- [5] C.C. Dollins, R.P. Tucker, "Irradiation-induced primary creep", *J. Nucl. Mat.* Vol 52, 1974, pp 277-288.
- [6] S. Oldberg, A.K. Miller, G.E. Lucas, "Advances in understanding and predicting inelastic deformation in zircaloy", *Proc. 4th int. symp. on zirconium in the nuclear industry*, ASTM STP 681, American Society for Testing and Materials, 1979, pp 370-389.
- [7] D. Lee, F. Zaverl, E. Plaza-Meyer, "Development of constitutive equations for nuclear reactor core materials", *J. Nucl. Mat.* Vol 88, 1980, pp 104-110.
- [8] J. Gittus, *Irradiation effects in crystalline solids*, Applied Science Publishers Ltd, London, 1978.
- [9] G.A. Maugin, *The thermomechanics of plasticity and fracture*, Cambridge University Press, Cambridge, UK, 1992.
- [10] T. Torimaru, T. Yasuda, M. Nakatsuka, "Changes in material properties of irradiated Zircaloy-2 fuel cladding due to short term annealing", *J. Nucl. Mat.* Vol 238, 1996, pp 169-174.
- [11] P. Robinet, "Etude experimentale et modelisation du comportement viscoplastique anisotrope du zircaloy 4 dans deux etats metallurgiques", PhD thesis no 442, 1995, Université de Franche-Comté, France.
- [12] G.S. Clevinger, B.L. Adams, K.L. Murty, "Analysis of irradiation growth and multi-axial deformation behavior of nuclear fuel cladding", *Proc. 4th int. symp. on zirc. in the nuclear industry*, ASTM STP 681, American Society for Testing and Materials, 1979, pp 189-201.
- [13] M. Nakatsuka, M. Nagai, "Reduction of plastic anisotropy of zircaloy cladding by neutron irradiation, (I) Yield loci obtained from Knoop hardness", *J. Nucl. Sci. Techn.* Vol 24(10), 1987, pp 832-838.
- [14] Y. Matsuo, "Creep behavior of zircaloy cladding under variable conditions", *Proc. 8th int. symp. on zirconium in the nuclear industry*, ASTM STP 1295, American Society for Testing and Materials, 1989, pp 678-691.
- [15] M.A. McGrath, "In-reactor creep behaviour of zircaloy-2 under variable loading conditions in IFA-585", OECD Halden Reactor Project report HWR-471, 1996.